universität wien

# MASTERARBEIT / MASTER'S THESIS

Titel der Masterarbeit / Title of the Master's Thesis

„Cell surface biotinylation of ApoER2 provides evidence of the existence of a possible new functional isoform"


verfasst von / submitted by

Roland Tresky, B.Sc.


angestrebter akademischer Grad / in partial fulfilment of the requirements for the degree of

Master of Science (MSc)

Wien, 2017 / Vienna 2017

| | |
|---|---|
| Studienkennzahl lt. Studienblatt / degree programme code as it appears on the student record sheet: | A 066 834 |
| Studienrichtung lt. Studienblatt / degree programme as it appears on the student record sheet: | Masterstudium Molekulare Biologie |
| Betreut von / Supervisor: | ao Univ.-Prof. DI Dr. Johannes Nimpf |

# Acknowledgement

I want to thank my supervisor ao. Univ.-Prof. Dipl.-Ing. Dr. Johannes Nimpf for his support and for giving me a chance to get insight into his scientific field.

Special thanks go to Paula Dlugosz, M.Sc. who supported me nine memorable months in the lab with her excellent expertise.

Special acknowledgement goes to Harald Rumpler for his technical support.

Finally, I must express my very profound gratitude to my parents and Magdalena for providing me with unfailing support and continuous encouragement throughout my years of study and through the process of researching and writing this thesis. This accomplishment would not have been possible without them. Thank you.

Affidavit:

I declare that my Master´s Thesis was independently authored by myself, using solely the referred sources and support. I additionally assert that this Master´s Thesis has not been part of another examination process.
Furthermore, I assure that the copies submitted by me (printed and electronically) are identical.

Vienna, January 17, 2018 _____

Signature of the author

# TABLE OF CONTENT


**1 INTRODUCTION ..... 12**

1.1. The LDL receptor family ..... 12

1.1.1. ApoER2 ..... 13

1.1.2. VLDLR ..... 14

1.1.3. The LDL pathway and cholesterol homeostasis ..... 14

1.1.4. Pathology of familial hypercholesterolemia ..... 16

1.2. Reelin: A ligand for ApoER2 and VLDLR ..... 17

1.2.1. Structure and function reelin ..... 17

1.2.2. The reelin signalling pathway ..... 17

1.2.3. The role of reelin and ApoER2 during brain development ..... 18

1.2.4. Pathomechanism of Alzheimer´s disease ..... 19

1.3. Aim of this thesis ..... 20

**2 METHODS ..... 22**

2.1. Cell culture ..... 22

2.2. Cloning of chimeric receptors ..... 22

2.3. Deletion of O-linked sugar domain of chimeric ApoER2 ..... 22

2.4. Extraction of plasmids ..... 24

2.5. Transfection ..... 24

2.6. RNA extraction ..... 25

2.7. Cell lysis and protein extraction ..... 25

2.8. Antibody coupling ..... 26

2.9. Co-immunoprecipitation ..... 26

2.10. Biotinylation ..... 27

2.11. SDS-PAGE and Western Blot ..... 27

2.12. Production of concentrated reelin and mock conditioned medium ..... 29

2.13. PCR ..... 30

2.14. Microscopy ..... 31

**3 RESULTS ..... 33**

3.1. ApoER2 detection in vivo reveals possible candidate for precursor. ..... 33

3.2. Glycosylation does not influence receptor stability on the cell surface ..... 34

3.3. Endogen expression von reelin mRNA in HEK 293 cells ..... 36

**4 DISCUSSION ..... 40**

**5 REFERENCES ..... 42**

## LIST OF FIGURES AND TABLES

**LIST OF FIGURES:**

Fig. 1. Overview of structural organization of the LDL receptor family ..... 13
Fig. 2. Schematic overview of the LDL pathway ..... 15
Fig. 3. The reelin signalling pathway ..... 18
Fig. 4. Overview of cortical development in early mouse brain ..... 19
Fig. 5. Western Blot „blotting sandwich“ ..... 29
Fig. 6. Production of reelin ..... 30
Fig. 7. Western Blots of ApoER2 HEK 292 and rat brain lysates ..... 33
Fig. 8. Surface biotinylation of ApoER2 ..... 36
Fig. 9. Confocal Microscopy of HEK293 cells ..... 37
Fig. 10. Detection of reelin with Western Blotting and PCR ..... 38
Fig. 11. Organization of the reelin gene. ..... 39

**LIST OF TABLES:**

Table 1. Quantity of DNA used for transfection for different sizes of cell culture dishes. ..... 25
Table 2. Composition of SDS gel ..... 28

| | |
|---|---|
| **A** | |
| α | alpha, anti |
| aa | amino acid |
| AD | Alzheimer's disease |
| ApoB | apolipoprotein B |
| ApoE | apolipoprotein E |
| ApoER2 | apolipoprotein E receptor 2 |
| APP | amyloid precursor protein |
| APS | ammonium persulfate |
| **B** | |
| BSA | bovine serum albumin |
| BisTris | Bis (2hydroxyethyl) amino-tris (hydroxymethyl) methan |
| bp | base pairs |
| **C** | |
| cDNA | complemantary DNA |
| CHO | Chinese Hamster Ovary |
| cm | centimeter |
| $CO_2$ | carbon dioxide |
| CR | Cajal-Retzius |
| cMCM | concentrated mock conditioned medium |
| cRCM | concentrated reelin conditioned medium |
| **D** | |
| Dab-1 | disabled-1 |
| DAPI | 4', 6-Diamidin-2-phenylindol |
| $ddH_2O$ | double distilled water |
| DMEM | Dulbecco´s Modified Eagle's Medium |
| DMSO | dimethyl sulfoxide |
| DNA | desoxyribonucleic acid |
| DNase | desoxyribonuclease |
| **E** | |
| EDTA | Ethylenediamine-tetraacetic acid |
| EtOH | ethanol |
| EphB | ephrinreceptor B |
| **F** | |
| FCS | fetal calf serum |
| FH | familial hypercholesterolemia |
| **G** | |
| GFP | green fluorescent protein |
| GSK3β | glycogen synthase kinase 3 beta |
| **H** | |
| h | hour |
| HCl | hydrochloric acid |
| HDL | high density lipoprotein |

## Abbreviations

| | |
|---|---|
| HEK | human embryonic kidney |
| HRP | horse radish peroxidase |
| **I** | |
| IgG | Immunoglobulin G |
| IP | Immunoprecipitation |
| **K** | |
| kDa | kilodalton |
| **L** | |
| LTP | long term potentiation |
| l | liter |
| LB | loading buffer |
| LDL | low density lipoprotein |
| LDLR | low density lipoprotein receptor |
| LRP-8 | Low-density lipoprotein receptor-related protein 8 |
| **M** | |
| M | molar |
| MCM | mock conditioned medium |
| µg | microgram |
| µl | microliter |
| µm | micrometer |
| mg | milligram |
| ml | milliliter |
| mM | millimolar |
| µM | micromolar |
| mRNA | messenger ribonucleic acid |
| **N** | |
| NaCl | sodium chloride |
| NHS | N-hydroxysuccinimide |
| NMDA | N-Methyl-D-Aspartat |
| **O** | |
| OLSD | O-linked sugar domain |
| **P** | |
| PI3K | Phosphoinositid-3-Kinasen |
| PEI | Polyethylenimin |
| PSD-95 | postsynaptic density protein 95 |
| **R** | |
| rel. mol. | relative molecular weight |
| **S** | |
| SD | sugar domain |
| SDS | sodium dodecyl sulfate |
| SDS-PAGE | sodium dodecyl sulfate polyacrylamide gel electrophoresis |
| SFK | Src family kinase |
| SP | subplate |

**T**

| | |
|---|---|
| TAE | Tris-acetate-EDTA |
| TG | triglycerides |
| TEMED | Tetramethylethylen-diamin |

**V**

| | |
|---|---|
| VLDL | very low density lipoprotein |
| VLDLR | very low density lipoprotein receptor |

## Abstract

The apolipoprotein E receptor type 2 (ApoER2, LRP-8) and very-low-density-lipoprotein receptor (VLDLR) are cell membrane receptors and part of the low-density lipoprotein receptor family. Members of this family take part in lipoprotein metabolism, cholesterol homeostasis and brain development. Therefore, they are involved in many diseases regarding the vascular system and the central nervous system. Defects of ApoER2 are involved in malformations of the brain and the development of Alzheimer's disease.

This study deals with the characterization of ApoER2 isoforms. It has been shown in a previous study that the ApoER2 receptor is integrated in lipid rafts, micro domains of the cell membrane which are enriched in glycosphingolipids and protein receptors. Previous analyses detected two variants of ApoER2. It was suggested that the smaller variant is the immature precursor which is unglycosylated and not yet integrated in the cell membrane. In this study, it could be demonstrated that this variant with a lower molecular weight is a hypoglycosylated isoform which is integrated into the plasma membrane of the cell and is not located in the lipid rafts. This isoform could be an interaction partner of the VLDL receptor which is also located in non-lipid raft regions of the membrane to from heterodimers. These findings suggest that the hypoglycosylated variant has a different function than the fully glycosylated variant of ApoER2 in the lipid raft fraction.

Der Apolipoprotein E Rezeptor Typ 2 (ApoER2, LRP-8) und der very low density lipoprotein Rezeptor (VLDLR) sind Zellmembranrezeptoren und Teil der LDL-rezeptorfamilie. Mitglieder dieser Familie nehmen am Lipoproteinmetabolismus, der Cholesterinhomöostase und der Gehirnentwicklung teil. Daher sind sie an vielen Erkrankungen des Gefäßsystems und des zentralen Nervensystems beteiligt. Defekte von ApoER2 sind an der Entwicklung von Hirnfehlbildungen und der Alzheimer-Krankheit beteiligt.

Diese Studie untersucht eine bislang schlecht charakterisierte Isoform von ApoER2. Es wurde in einer früheren Studie gezeigt, dass der ApoER2-Rezeptor in lipid rafts integriert ist, welche mit Glycosphingolipiden und Proteinrezeptoren in der Zellmembran angereichert sind. In früheren Analysen wurden immer zwei Rezeptorvarianten in vitro detektiert. Es wurde angenommen, dass die kleinere Variante der unreife Precursor (Vorläuferprotein) von ApoER2 ist, welcher nicht glykosyliert und nicht in die Zellmembran integriert ist. In dieser Studie konnte gezeigt werden, dass diese zweite Rezeptorvariante mit einem niedrigeren Molekulargewicht eine möglicherweise hypoglykosylierte Isoform ist, die in die Plasmamembran der Zelle integriert wird und nicht in den lipid rafts zu finden ist. Diese Isoform kann als Wechselwirkungspartner des VLDL-Rezeptors dienen, der auch in nicht-lipid raft Regionen der Zellmembran lokalisiert ist um Heterodimere zu bilden. Dies deutet darauf hin, dass diese Variante eine abweichende Funktion haben könnte als der ApoER2 in der lipid raft Fraktion.

# 1 Introduction

In today's affluent society, diseases affecting the cardiovascular system became a frequent problem in public health concerns. Hypercholesterolemia is such a risk factor [Biggerstaff, Wooten; 2004]. High levels of blood cholesterol are accumulating over time in the tissue or in the vascular walls, causing arthrosclerosis. High levels of cholesterol are often the result of poor diets. In addition, genetic mutations have been identified to increase cholesterol blood levels. A mutation in the LDL receptor is the major cause of "Familial Hypercholesterolemia", preventing the uptake of LDL into the cell [Durrington; 2003].

The LDL receptor belongs to a large family of homologous proteins (the LDL receptor family). ApoER2 and VLDLR are signaling receptors and orchestrate migration of neuroblasts during brain development through binding their ligand reelin. Reelin is expressed by Cajal-Rezius-cells and acts as a stop signal for migrating neurons, thus establishing formation of cortical layers [Honda, et al; 2011]. Consequently, dysfunction or altered expression of reelin and its receptors promote the development of neurological diseases such as schizophrenia [Ishii et al; 2016] and Alzheimer's disease [Botella-López, et al; 2006].

## 1.1. The LDL receptor family

The low-density lipoprotein receptor is an evolutionary conserved group of cell surface receptors that serve as signal transducers in neuronal migration, cholesterol homeostasis, and many more processes [Nykjaer, Willnow; 2002] [Li, et al; 2001]. Some important members of the LDL family are: Low-density-lipoprotein receptor (LDLR), Low-density-lipoprotein receptor-related protein 1 (LRP1 or LRP), Low-density-lipoprotein receptor-related protein 2 (LRP2 or megalin), Low-density-lipoprotein receptor-related protein 8 (LRP-8 or ApoER2), Very-Low-density-lipoprotein receptor (VLDR or LR8), Low-density-lipoprotein receptor-related protein 5 and 6 (LRP5, LRP6). [Nykjaer, Willnow; 2002]

Members of the LDLR family share common structural motifs. The internalization signal (NPxY motif → Aspargin – Prolin – x – Tyrosine) located at the C-terminal domain mediates the clustering of the receptor into coated pits (regions within the plasma membrane surrounded by clathrin for endocytosis). On the extracellular side, some of the receptors contain a short serine and threonine rich region which can be modified with O-linked sugars, the so called O-linked sugar domain (Fig. 1) [Schneider, Nimpf; 2003] [Nykjaer, Willnow; 2002].

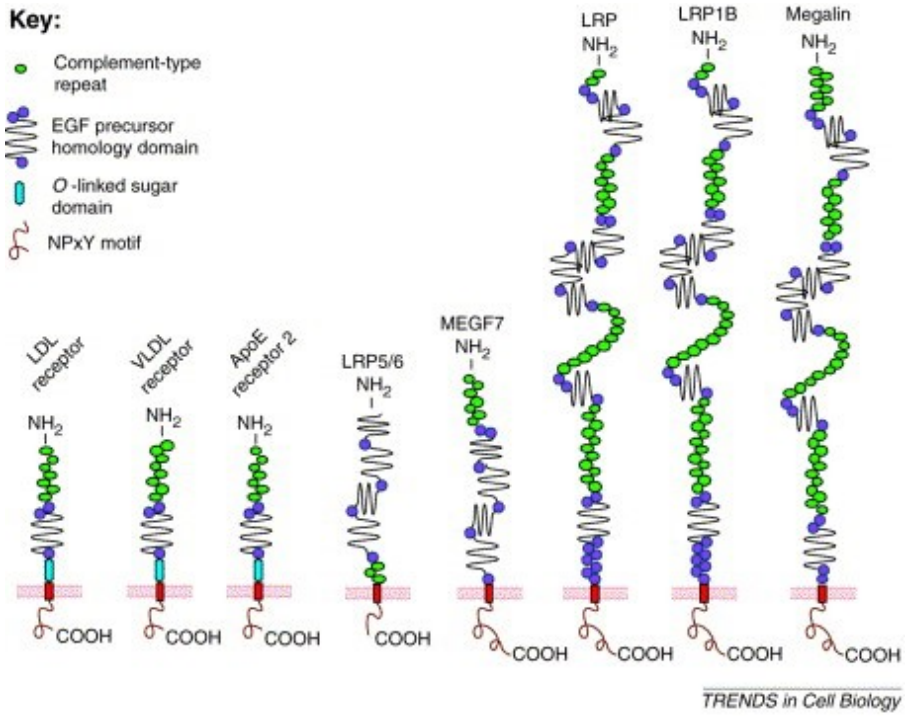


**Fig. 1.** Overview of structural organization of the LDL receptor family. The N-Terminal complement type repeat (or LDL receptor Type A repeat) is responsible for ligand binding, whereas the EGF precursor homology domain (LDL receptor Type B repeat) is important for the release of ligands into the endosome [Figure taken from Nykjaer, Willnow; 2002].

### 1.1.1. ApoER2

ApoER2 consists of 870 amino acids and is similar to the VLDL receptor. The gene encoding for ApoER2 contains exons, coding for 8 Ligand binding repeats (LBR). Only five of them are present in the final protein, due to alternative splicing. The O-linked sugar domain contains 89 amino acids, the transmembrane contains 23 amino acids and the cytoplasmic intracellular tail contains 115 amino acids. Furthermore, unlike other members of the LDL receptor family, the C-terminal domain has a proline rich region due to alternative splicing of Exon 19 which promotes interaction with other proteins like PSD-95 or c-jun N terminal kinase interacting proteins [Reddy, et al; 2011] [Stockinger, et al; 2000].

The main function of ApoER2 is in the reelin-signaling-pathway during brain development. Interestingly, the knockouts of ApoER2 or VLDLR in mice have only minor effects. In ApoER2 $^{-/-}$ and VLDLR$^{-/-}$ mice a smaller cerebellum could be observed. Furthermore, male ApoER$^{-/-}$ mice showed reduced fertility. Interestingly, ApoER2 knockout affects preferentially the development of the neocortex, whereas the VLDLR knockout affects preferentially the development of the cerebellum. Nevertheless, both receptors are

required for neuronal migration and only the absence of both receptors causes the exact anatomical phenocopy of the reeler mutation and only mice lacking both receptors showed a neurological phenotype. This indicates that VLDLR has overlapping functions with ApoER2 [Trommsdorf, et al; 1999].

### 1.1.2. VLDLR

The VLDL receptor is similar to the LDL receptor. However, VLDLR has 8 Ligand binding repeats and LDLR only 7. Four alternatively spliced variants of VLDLR are known until now. The full length receptor VLDLR-I lacks none of its Exons. The VLDLR-II variant lacks Exon 16 containing the O-liked sugar domain. VLDLR-III lacks Exon IV and VLDLR-IV lacks both Exon 4 and Exon 16. It is crucial in cholesterol homeostasis and neuronal migration during brain development [Go, Mani; 2012] [Reddy, et al; 2011].

Before the discovery of VLDLR only the LDL receptor was known. Experiments with polyclonal antibodies against LDL revealed a LDL-receptor homologue with the relative molecular weight of 95 kDa in hen oocytes. This LDL-receptor homologue was later identified as the VLDL receptor which is able to bind ApoB100 and thus is responsible for VLDL uptake into the growing oocyte. Furthermore, it is the receptor for many other ligands such as vitellogenin (a yolk precursor) and alpha-2-macroglobulin (a protease inhibitor). In summary, its ligands and therefore the VLDLR are necessary for oocyte development in egg laying species. [Stifani S, et al; 1991] [Hayashi, Nimpf, Schneider 1989]

### 1.1.3. The LDL pathway and cholesterol homeostasis

Cholesterol is an important part of the cell plasma membrane and a precursor for hormones. Through its lipophilic and hydrophobic nature it is bound to lipoproteins, so it can be transported through the blood stream. Cholesterol is packaged into so called chylomicrons in the intestines and is then transported to the liver. There, it gets incorporated into VLDL and gets released into the bloodstream. HDL takes up cholesterol from the tissue and brings it back to the liver. In general, lipoproteins are built up of cholesterol, triglycerides, phospholipids and proteins (e.g. apolipoprotein E) (Fig. 2) [Go, Mani; 2012] [Durrington; 2003].

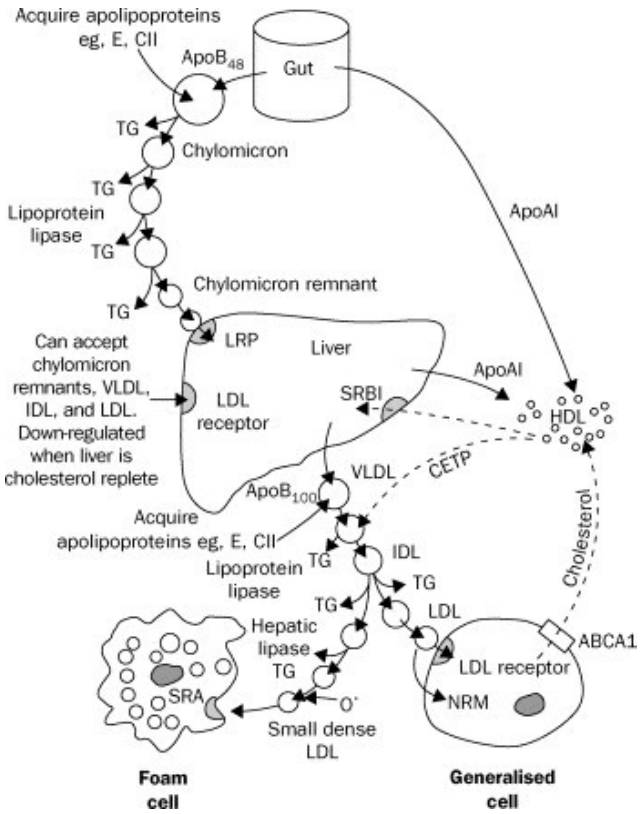


**Fig. 2.** Schematic overview of the LDL pathway. Triglycerides (TG) and cholesterol is incorporated by the gut and packaged into chylomicrons (have $ApoB_{48}$ as structural lipoprotein). On their way to the liver, they acquire other apolipoproteins, like ApoE, and lose triglycerides through interaction with lipases. These triglyceride-depleted chylomicrons are called chylomicron-remnant. In the liver the triglycerides and cholesterol gets packed together with $ApoE_{100;}$ ApoE and phospholipids to form VLDL. VLDL leaves the liver and is converted to LDL due to the loss of triglycerides. LDL is now taken up by all cells which need cholesterol by LDL-receptor mediated endocytosis. HDL transports excessive amounts of cholesterol back to the liver or it gets taken up by macrophages and form so called foam cells [Figure taken from Durrington; 2003].

Cholesterol can be endogenously synthesized by all cells, but it is mainly produced in the liver. Starting from acetyl-CoA, two condensation reactions form HMG-CoA. Afterwards, HMG-CoA is reduced by HMG-CoA reductase to mevalonate. This is the speed-determining step and the one where pharmaceutical drugs like statins are applied to inhibit cholesterol production in case of pathological high cholesterol levels. In a series of additional steps, cholesterol is produced [Nes; 2011].

### 1.1.4. Pathology of familial hypercholesterolemia

Familial hypercholesterolemia is the phenomenon of abnormal high levels of cholesterol at young age resulting in sudden death due to arteriosclerosis. Heterozygote FH is one of the most common genetic diseases with a prevalence of 1:500. In contrast, the homozygote FH has a prevalence of 1:1,000,000 and is clinically more severe. Overall, the major causes to develop this disease are mutations in the LDLR, ApoB or PCSK9 gene [Raal, Santos; 2012]. The dysfunction of the LDL receptor can have multiple reasons. First, aberrations within the promotor sequence leading to a lack of expression. Furthermore, maturation of the protein can be faulty or the binding of the ligand is defective. Additionally, the mechanism of endocytosis after binding LDL or recycling the receptor can be defective [Marais; 2004].

Defects in the $ApoB_{100}$ cause a similar phenotype. It is a large protein of 550 kDa in size and serves as a ligand for cellular uptake of LDL via the LDL receptor resulting in elevated levels of cholesterol [Marais; 2004]. There exist several other mechanisms, like PCSK9 mutation, which will be not discussed here in detail.

The final outcome of rising blood cholesterol levels is the formation of xanthomas (aggregations of cholesterol and lipids caused by foam cells) and the formation of atherosclerosis. LDL in the blood stream is able to infiltrate the intima by slipping between endothelia cells. There, it can be modified by oxidation processes that can affect either its proteins as well as its lipids. Furthermore, it can be modified by malondehyde attachment. In case of high LDL levels, a large quantity accumulates in the intima. The appearance of modified LDL triggers vascular homeostasis and a series of inflammation responses, like chemokine secretion and increased adhesion molecule expression. These events cause recruitment of monocytes, stimulation of macrophages and the migration of smooth muscle cells into the intima. The activated macrophages incorporate the modified LDL via their scavenger receptors. Excessive LDL uptake by macrophages results in formation of so called foam cells. Accumulation of foam cells and the increased migration of smooth muscle cells cause the intima to swell and narrows the blood vessel (plaque). This is an ongoing process until the integrity of the endothelial is compromised. Thrombocytes in the bloodstream come in contact with the collagen in the intima and blood coagulation is triggered. The activated thrombocytes clot together and form a thrombus. The size of the thrombus expands until it completely seals the blood vessel or it gets carried away with the blood

stream until it clogs a smaller vessel (infarct) [Parthasarathy, at al; 2010] [Zmysłowski, Szterk; 2017] [Peng, et al; 2017].

## 1.2. Reelin: A ligand for ApoER2 and VLDLR

Reelin is an extracellular glycoprotein which plays a role in early brain development by guiding migrating fibroblasts. Furthermore, it is also expressed in adult brain where it has different functions (e.g. modulation of synaptic plasticity). During the development of the brain, reelin is produced by Cajal-Retzius cells, located in the marginal zone, and secreted into the extracellular space. It consist of 3641 amino acids containing a serine protease domain which is responsible for its cellular function [Weeber, et al; 2002] [Quattrocchi, et al; 2002].

### 1.2.1. Structure and function of reelin

Reelin has an apparent molecular weight of 450 kDa. Its DNA contains a CG rich promotor without a TATA box. The protein itself has a signal peptide domain similar to F-spondin followed by a domain which is unique for reelin (segment H) between amino acid 191 and 500. This region is recognized by antibodies 142, G10 and CR50 [Tissir, Goffinet; 2003]. Furthermore, eight reelin-repeats alternate with EGF like motifs [Quattrocchi, et al; 2002].

### 1.2.2. The reelin signaling pathway

The reelin signaling pathway is evolutionary conserved and important for brain function and development. When reelin is bound, it initiates the clustering of VLDL receptor and ApoER2. The NPxY motif of both receptors interacts with Dab-1 (intracellular signaling protein), which becomes phosphorylated upon clustering of the receptors and activates SFK. SFK in turn phosphorylate the NMDA receptor, thus inhibiting its endocytosis. Once glutamate is bound to the NMDA receptor, it gets activated in presence of PSD-95 (requires Exon 19 of ApoER2) and facilitates $Ca^{2+}$ influx into the cell leading to increased long term potentiation (LTP). LTP is a form of synaptic plasticity, involved in learning and memory. Furthermore, Dab-1 leads to activation of PI3K, thus inhibiting cofilin, which results in actin polymerization (important for cell migration) and spine growth. Additionally, PI3K activation

inhibits tau hyperphosphorylation through GSK-3β which is responsible for neurofibrillary tangles in Alzheimer's disease AD (Fig. 3) [Lane-Donovan, Herz; 2017].

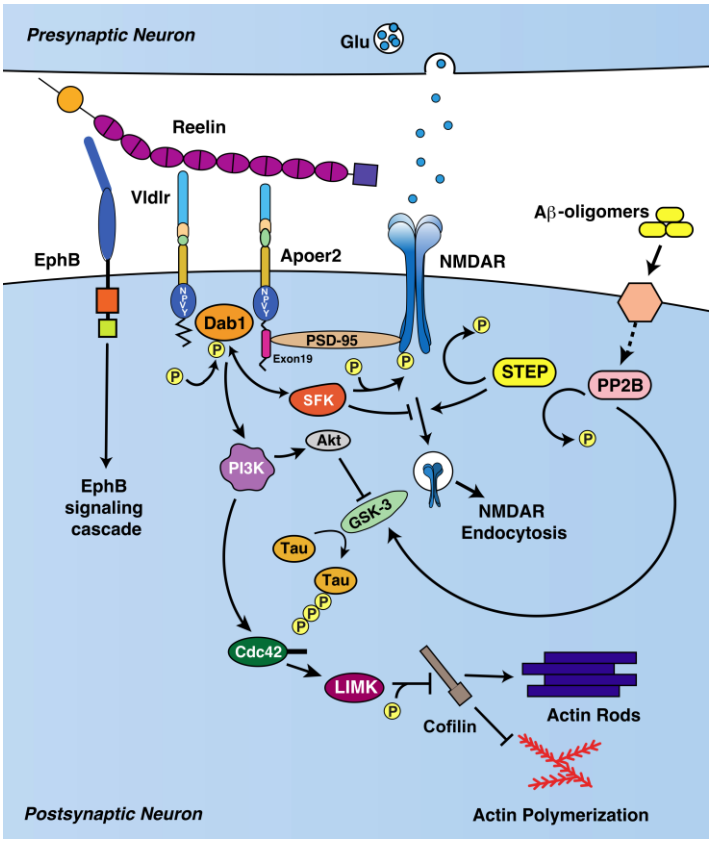


**Fig. 3.** The reelin signalling pathway. NMDAR: is an ion channel that is activated by binding of glutamate (Glu). Glutamate is an amino acid that is released from a presynaptic neuron into the presynaptic junction for signal transmission to the postsynaptic neuron. EphB: responsible for polarisation and growth of axons. Aβ oligomers promote NMDAR endocytosis via activation of STEP [Figure taken from Rohani, et al; 2011].

### 1.2.3. The role of reelin and ApoER2 during brain development

The cerebral cortex of a mouse embryo develops from day ten to day 17 [Haydar, et al; 1996].Neuronal stem cells form the preplate and start to differentiate into Cajal Retzius (CR) cells and subplate cells (SP). CR cells start to secrete reelin which orchestrates neuronal migration. Subplate neurons start to migrate along the fibers of glia cells towards the marginal zone until they reach the reelin secreting CR cells. Reelin might act here as a stop signal [Zaho, Frotscher 2010]. While the SP cells start to differentiate, the CR cells move away and form the cortical plate and thereby increase telencephalic wall thickness. Early neurons form the cortical preplate by moving along glia fibers until they reach reelin

secreting CR cells, stop and dissociate from glia fibers. These cells need either ApoER2 or VLDLR to receive the reelin signal. In case of reelin absence (or both receptors) the SP cells are not prevented from stopping by reelin signaling and therefore do not dissociate from the glia fibers. Consequently, younger neurons are not able to pass by older ones and the preplate is not split. This results in a reversed formation of the cortex structure (Fig. 4) [Tissir, Goffinet; 2003] [Frotscher; 1998].

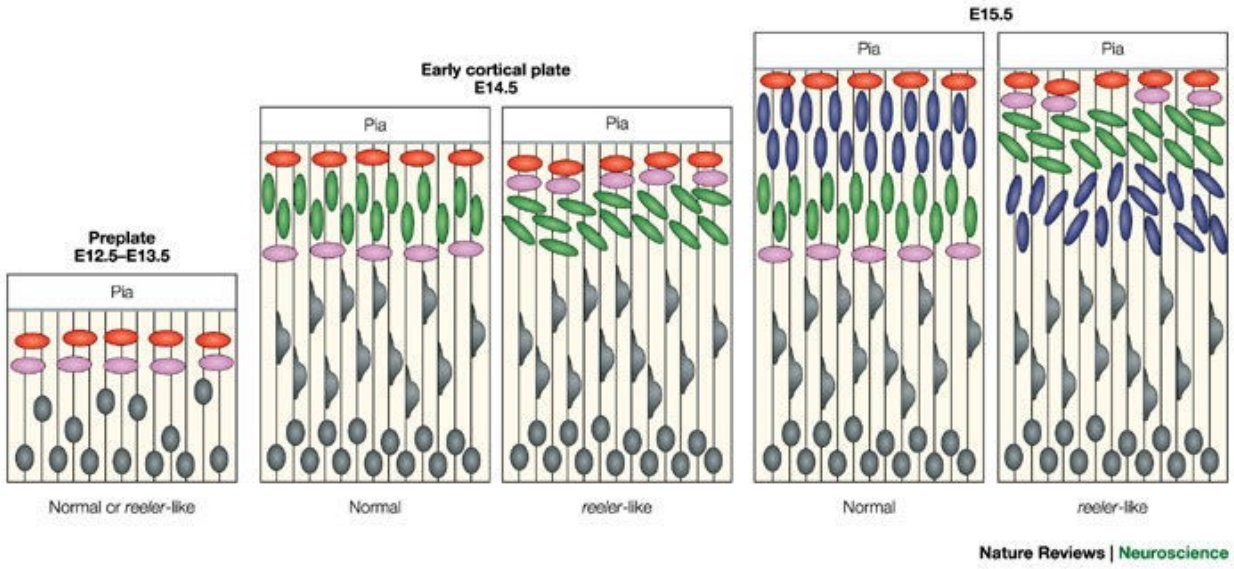


**Fig. 4.** Overview of cortical development in early mouse brain. Right under the pia the marginal zone including the reelin secreting CR cells (Red) is located. The cortical plate is formed in between the CR cells and the germ cells (pink). Below the germ cells is the intermediate zone which contains the glia fibers (vertical lines) and the migrating neurons (grey). On the bottom is the ventricular zone where the migrating neuroblasts are produced from neuronal precursor cells. Precursor cells differentiate into SP cells which now migrate along the glia fibers until they reach the reelin secreting CR cells. They dissociate from the fibers and descending neurons are able to move past the older neurons. Thereby, the cortex gets divided into six cortical layers. In the reeler mutant, the SP cells do not receive the reelin stop signal and do not dissociate from the fibers. This causes the cells to pile up and the reversion of cortical layers [Figure taken from Tissir, Goffinet; 2003].

### 1.2.4. Pathomechanism of Alzheimer´s disease

Currently, there are two pathological aspects that are associated with the development of Alzheimer's disease. One is the formation of amyloid β plaques causing

neuronal dysfunction. The other are insoluble aggregates of tau protein (a microtubules stabilizing protein) which cause the formation of neurofibrillary tangles and disrupt the function of neurons [Ballard, et al; 2011].

Amyloid β precursor (APP) is cleaved by β and γ secretase in amyloid β peptides which form oligomers. These oligomers form plaques inside neurons and extracellularly and are supposed to be toxic, thus inducing cell death or neuronal dysfunction. It is hypothesized that they also have a negative effect on tau protein, leading to its hyperphosphorylation, causing it to aggregate and form so called neurofibrillary tangles [Ballard, et al; 2011].

However, there are more genetic risk factors than APP or tau. Besides mutations in the γ secretase or GSK3β gene, a variation of the ApoE gene (ApoE4) has been identified as a major risk factor increasing the probability of developing AD three (one allele of ApoE4) to seven times (homozygous for the apoE4 allele) [Ballard, et al; 2011]. This ApoE isoform is present in 20 % of the population. Its primary function is the transport of cholesterol and triglycerides in chylomicrons, VLDL and HDL particles. In terms of AD, it might play a role in amyloid β clearance. Nevertheless, the exact mechanism and function remains unknown [Lane-Donovan, Herz; 2017].

It has also been shown that reelin levels in AD patients are reduced, which results in reduced LTP induction. Under normal conditions, reelin is able to interact with APP by increasing interaction with Dab-1 and ApoER2. This leads to an increased cleavage of APP by α secretase into non-toxic amyloid β fragments [Yu, et al; 2016].

## 1.3. Aim of this thesis

Conflicting results obtained in previous studies exist about the nature of the different variants of ApoER2 seen in whole brain extracts, derived from mice. Two distinctive bands with a relative molecular weight of 130 kDa and 115 kDa can be observed. It was claimed that this 115 kDa ApoER2 is the precursor [Burrell, et al; 2014]. In addition, brain lysates of mice with an additional band at approximately 100 kDa were also observed [Wasser, et al; 2014]. Expression studies and pulse chase experiments, performed in heterologous cell systems, were not able to fully resolve the nature of these variants. Previous biotinylation experiments detected the 130 kDa and 115 kDa bands at the cell membrane. It was interpreted in a way, in which the immature receptor was able to reach the cell surface due to overexpression [Burrell, et al; 2014]. Pulse chase studies in our laboratory verified that the

115 kDa band is not the precursor, but it also could not detect the 100 kDa band that is visible in brain lysate [Dlugosz manuscript in preparation].

ApoER2 shows three clearly distinguishable bands in rat brain tissue with relative molecular masses of 130 kDa, 115 kDa and 100 kDa (Fig. 7). Previous studies have led to the assumption that the 115 kDa fragment could be an additional isoform of ApoER2. Since an immature receptor is considered to have no glycosylation modification, experiments were carried out with a full length ApoER2 and a truncated version, where the o-linked sugar domain was missing (ApoER2Δ16). This approach allows the investigation of the size of a potential precursor or the possible presence of an unknown isoform.

# 2 Methods

## 2.1. Cell culture

HEK293 and NIH3T3 lines were cultured in DMEM (Thermo Fisher Scientific #11965092) supplemented with 10% FCS. All cell lines were grown at 37°C and 5% CO2. Cell lines expressing chimeric proteins were grown under the same conditions. CHO cells were cultured in Ham´s F12 medium supplemented with 10% FCS (Lonza Group AG #BE12-615F).

## 2.2. Cloning of chimeric receptors

Preexisting chimeric ApoER2 (pmGFP_ApoER2, pmCherry_ApoER2, pClneo_ApoER2), ApoER2Δ16 (pClneo_ApoER2Δ16) and VLDLR (pmGFP_VLDLR) were provided by Paula Dlugosz.

## 2.3. Deletion of O-linked sugar domain of chimeric ApoER2

For deletion of the glycosylation domain of the ApoER2 receptor, a pre-existing plasmid containing the full length receptor was used. The deletion itself was carried out with the Thermo Scientific Phusion Site-Directed Mutagenesis Kit (Thermo Fisher Scientific, #F-541). The following primers were used to delete the O-linked sugar domain (OLSD): ApoER2ΔSDFW (5´-TCC ACC CCG AGC CCT GCT ACC AGC a-3´) and ApoER2ΔSDBW (5´-CTG AGG TGC TCG GTA GCA TCT CTT CA-3´). The first round of PCR, to delete the SD out of the full length plasmid, was performed with the Thermo Scientific Phusion Hot Start II High-Fidelity DNA Polymerase (Thermo Fisher Scientific, #549S). In a total volume of 50 µl, 1 µl (≈4 ng) of pmGFP_ApoER2 plasmid DNA were mixed together with 10 µl of 5 x Phusion HF Buffer, 1 µl of dNTPs (10 mM), 1.5 µl DMSO, 2.5 µl of forward and reverse primer each (10 µM) and 0.5 µl of Phusion Hot Start II Polymerase (2 U/µl). The remaining volume was filled up with nuclease free $H_2O$. ApoER2ΔSD PCR was run at 98°C for 30 seconds followed by 35 cycles of 98°C for 10 seconds, 72°C for 105 seconds and finally 72°C for 10 minutes. Negative controls were included. 1 µg of PCR (mixed with 2 µl DNA gel loading dye, Thermo Fisher Scientific, #R0611) were analyzed on an agarose gel 1% in 1 x TAE Buffer (40 mM Tris, 0.57 % CH3COOH, 0.5 M EDTA pH 8.0) with 3 µl Midori green (Nippon genetics #MG05) and run for an hour with 100 V.

Afterwards, the linear PCR products were ligated. Therefore, 1 µg of PCR product was mixed with 2 µl of 5 x Rapid Ligation Buffer, 0.5 T4 Ligase and adjust the volume to 9.5 µl with nuclease free $H_2O$. The mixture was quickly centrifuged and incubated for 5 min at RT. Then, the solution was quickly put on ice and 50 µl of DH5α™ competent cells (Thermo Fisher Scientific, # 18265017) were added. After an incubation time of 30 min on ice, the bacteria were heat shocked by putting the solution for 1 min on 42°C and then on ice again for 10 min. Then, 1 ml of LB medium (tryptone 10 g, yeast extract 5 g, NaCl 10 g, agar 15 g for plates, pH 7.0 adjusted with NaOH) supplemented with kanamycin (100 µg/ml) was added and incubated for 1 h at 37°C on the dry bath incubator under constant shaking (180 rpm). After centrifugation (3000 x g for 5 min), the bacteria was plated on LB medium supplemented with kanamycin.

The next day, 5 round bottles containing LB medium supplemented with ampicillin (100 µg/ml) were prepared. E. coli colonies were picked with a pipetted tip and transferred into a round bottle. Afterwards, they were incubated again overnight at 37°C and constant shaking 180 rpm.

For the extraction of the plasmid the PureYield™ Plasmid Miniprep System was used (Promega, # A1223). One of the cultures could be used to create a viable bacterial stock. Therefore 850 µl of culture was added to 150 µl of glycerol and stored at -80°C. The other four cultures bottles were used for plasmid extraction. To increase the yield, 2 ml of each round bottle tube was pipetted into a 2 ml microtube and centrifuged for 30 s at maximum speed. The supernatant was discarded and the bacterial pellet was resuspended in 600 µl of TE Buffer. The bacteria were lysed with 100 µl Cell Lysis Buffer. The solution was mixed thoroughly and 350 µl of ice cold Neutralization Buffer was added. The mix was vortexed and centrifuged at maximum speed for 3 min. Then, the supernatant was transferred on a PureYield™ Minicolumn attached to a Vac-Man™ Laboratory Vacuum Manifold (Promega, # A7231) and the lysate was pulled through the column by applying vacuum. Afterwards, the membrane of the column containing the plasmid, was treated with 200 µl of Endotoxin Removal Wash and then with 400 µl of Wash Solution. To dry the membrane the column was placed into a collection tube and centrifuged for 1 min at maximum speed. A 1.5 ml microtube was placed into the Spinlock II Adapter attached to the Vac-Man™ Laboratory Vacuum Manifold. Then the column with the dried membrane was put on top of the microtube and 30 µl of nuclease free $H_2O$ was added. After incubation of 1 min the vacuum

was applied again to elute the plasmid from the membrane. The yield of purified plasmid was analyzed with a NanoDrop™ 2000c Spectrophotometer (Thermo Fisher #ND-2000C).

For new plasmid supply, an Erlenmeyer flask with 300 ml LB supplemented with kanamycin (100 µg/ml) was inoculated with bacterial stock from -80°C by scratching a bit from the frozen stock with a pipette tip. Then it was incubated overnight at 37°C and constant shaking at 180 rpm. For plasmid extraction the PureYield™ Plasmid Midiprep System (Promega, # A2492) was used (see section 2.4 Extraction of plasmids).

## 2.4. Extraction of plasmids

The bacterial stock grown overnight was centrifuged at RT for 10 min with 5,000 g. The supernatant was discarded and the cells were resuspended in 6 ml of Resuspension Buffer. Afterwards, 6 ml of Cell Lysis Buffer was added, mixed thoroughly and incubated at RT for 3 min. Then, 10 ml Neutralization Buffer were added, inverted at least 5 times and then centrifuged for 30 min with 8,000 g. In the meanwhile, the column stack was assembled. PureYield$^{TM}$ Clearing Column was put on top of a PureYield$^{TM}$ Binding Column and attached to a Vac-Man$^{TM}$ Laboratory Vacuum Manifold. The lysate was carefully decanted into Clearing Column without disturbing the cell debris pellet. The Clearing column was removed and the membrane of the Binding Column was treated at first with 5 ml Endotoxin Removal Wash and then with 20 ml of Column Wash Solution. The membrane was dried by leaving the vacuum on until the ethanol odor is completely vanished. Finally, the plasmid got eluted into a 1.5 ml microtube with 600 µl of nuclease free $H_20$ after an incubation time of 1 min.

## 2.5. Transfection

Seeded cells were grown until a confluence of about 70 %. The next day a transfection reagent mix was prepared. Therefore x µl of DNA (Table 1) was added to a microtube containing 3 times the volume of DNA of PEI (1µg/µl, pH4.5 in PBS) plus 100 µl of medium (without FCS). Afterwards, the mixture was incubated for 15 min at RT and added to the corresponding plate.

**Table 1.** Quantity of DNA used for transfection for different sizes of cell culture dishes.

| Plate size | DNA [ng] | Surface area [$cm^2$] |
|---|---|---|
| 3,5 cm | 2,000 | 10 |
| 6 cm | 4,000 | 20 |
| 10 cm | 10,000 | 60 |
| 15 cm | 20,000 | 140 |
| 6 well | 2,000 | 10 |
| 12 well | 1,000 | 4 |
| 24 well | 500 | 2 |

## 2.6. RNA extraction

Total RNA extraction was carried out with the peqGold Trifast™ RNA extraction agents (pepLab #30-2030), according to the manufacturers protocol. The medium was aspirated and 5.5 ml (for 10 cm dish) of peqGold Trifast™ solution was added (1ml per $10cm^2$). After an incubation time of 5 min at RT the solution was transferred into a new tube (50 ml Falcon Tube). Then 1.1 ml of pure chloroform was added, mixed thoroughly and incubated for 10 min at RT. For phase separation the solution was centrifuged at 3,260 x g for 30 min at 4°C (12,000 x g for 5 min according to the manufacturer). Afterwards, the aqueous phase containing RNA (top phase) was pipetted into a new tube (15 ml Falcon tube) and 2.75 ml isopropanol was added (0.5ml isopropanol per ml peqGold Trifast™). The solution was then homogenized and incubated for 15 min on 4°C. It can also be stored at lower temperatures (-80°C) and overnight if necessary. Subsequently, the solution was 3,260 x g for 30 min at 4°C and the isopropanol was removed. 1ml of 75 % Ethanol was then added to the RNA residue, mixed and centrifuged at 3260 x g for 30 min at 4°C. This step was repeated once before the RNA pellet was dissolved in 100 µl in nuclease free $H_2O$.

## 2.7. Cell lysis and protein extraction

After aspiration of the old medium, the cell layer was once washed with ice cold PBS (140 mM NaCl, 2.5 mM KCl, 8.1 mM $Na_2HPO_4$, 1.5 mM $KH_2PO_4$, pH 7.3). Then, 300 µl (10 cm dish) of lysis solution (NP40 lysis Buffer (150 mM NaCl, 1 % NP-40, filld up with 50 mM Tris pH 7), 1 x cOmplete™ Protease Inhibitor Cocktail (Sigma-Aldrich, #CO-RO), 5mM EDTA,) were added to the cells and incubated for 15 min on ice. Cells and lysate were collected with a cell

scratcher and pipetted into a new 1.5 ml microtube. Cell debris was spun down at 4°C with max speed. The protein-containing supernatant was transferred in a new microtube and stored at -80°C. For in vivo protein extraction 1-2 ml of lysis solution was added to a microtube contain one rat brain (embryonal day 17).

In order to measure protein concentration, the Pierce™ BCA Protein Assay Kit (Thermo Fisher #23225) and a NanoDrop™ 2000c Spectrophotometer was used following the manufactures instructions.

## 2.8. Antibody coupling

In order to couple IgG antibodies to beads, 1.5 ml of Protein A Sepharose™ (abcam # ab193256) and 1.5 ml of antibody solution (α6A6) were gently mixed together and incubated at RT for 2h on a rotator. Afterwards, beads were washed by spinning them down and 10 ml 0.2 M sodium borate pH9 were added. The washing step was repeated at least once. Then, the beads were resuspended in 10 ml solution of 20 mM dimethyl pimelimidate in 0.2 M sodium borate (freshly made) and incubated for 1h at RT on a rotator. Subsequently, the beads were spun down and washed one time with 10 ml of 0.2 M ethanolamine pH8 (freshly made). The beads were spun down again and the ethanolamine supernatant was discarded. Now the beads were incubated with 10 ml of ethanolamine 0.2 M pH8 for 2h at RT on a rotator. Finally, the beads were spun down and washed with 10 ml of 100 mM glycine pH 3. Additionally, they were washed four times with PBS and a last time with a PBS/$Na_3N$ solution (3 M $Na_3N$ diluted 1:1,000 in PBS). The antibody coupled beads were stored in PBS/$Na_3N$ solution at 4°C. All centrifugation steps were carried out with 500 x g for 1 min.

## 2.9. Co-immunoprecipitation

60 µl of antibody mouse anti-VLDLR α6A6 (Santa Cruz Biotechnology Inc., #sc-18824) coupled protein A beads were added to rat brain lysate and incubated overnight at 4°C at a rotator.

The next day, an SDS gel was prepared (see section 2.11 SDS-PAGE and Western Blot). The beads were spun down with 500 g for at 4°C. Supernatant was aspirated and stored at -80°C. Subsequently, 0.5 ml of fresh lysis buffer was added to the beads, mixed well and centrifuged with 500 g at 4°C. This washing step was repeated at least twice. In order to elute bound protein from the antibody, 60 µl of 4x loading buffer was added and

incubated for 10 min at RT on a rotator. Then 6 µl of 1 M Tris was added to the beads, mixed and boiled for 10 min at 95°C. Finally, the beads were spun down before SDS-PAGE.

## 2.10. Biotinylation

Transfected cells were washed twice with ice cold PBS. Afterwards, 2.9ml (10 cm dish) or 0.6 ml (3.5 cm dish) of EZ-Link™ Sulfo-NHS-SS-Biotinsolution (0.5 mg/ml pH 7.4) (Thermo Fisher Scientific #21331) was added and incubated on ice for 1h. After incubation, cells were carefully washed three times with cold quenching solution. Between each washing step, 5 minutes incubation time was maintained. Then cells were lysed with 1,000 µl (10 cm dish) or 200 µl (3.5 cm dish) IP buffer (1% Triton, 5mM EDTA, 1x Pierce™ Protease Inhibitor Tablets Thermo Fisher Scientific #88266, Phosphatase Inhibitor Cocktail 2 Sigma # P5726) and incubated on ice for 10 min. Lysate is then transferred to a microtube and centrifuged at 4°C with max speed (≈ 14,000 rpm) for 10 min. Supernatant was transferred into a new microtube. Approximately 25-50µl was used for protein concentration measurement and as lysate samples. The rest was mixed with 250 µl (10 cm dish) or 75 µl (3.5 cm dish) of Pierce™ NeutrAvidin™ Agarose beads (Thermo Fisher Scientific #29200) and rotated overnight at 4°C.

The next day, beads were spun down at 4°C for 10 min with 5,000 rpm. The supernatant was discarded and the beads were washed with 1 ml of IP buffer at least three times. Each washing step was performed at 4°C and incubated 5 min on a rotator. Finally, the supernatant was removed and 60 µl (10 cm dish) or 30 µl (3.5 cm dish) of 4x loading buffer (40 % glycerol, 240 mM Tris/HCl pH 6.8, 8 % SDS, 0.04 % bromophenol blue, 5 % beta-mercaptoethanol) was added and boiled for 10 min at 65°C. After an additional centrifugation step, supernatant was used for SDS-PAGE [Huang, 2012].

## 2.11. SDS-PAGE and Western Blot

After assembling the gel electrophoresis apparatus all components for the separating gel, except APS and TEMED, were mixed together in a 50 ml falcon tube. The same was done with the stacking gel. Shortly before pouring the gel, APS and TEMED was added to the stacking gel solution and vortexed (Table 2). Afterwards, approximately 4.5 ml of the mixture was pipetted in the gel chamber. The gel was then covered with a little isopropanol, to ensure a bubble free and straight gel surface. After the polymerisation of the separating gel,

APS and TEMED was added to the stacking gel mixture and poured on top of the stacking gel. Finally, a 10 well SDS comp was inserted. Gradient gels were poured by mixing a 4.5% gel (2.925 ml $H_2O$, 0.775 ml 30% acrylamide mix) with a 18% gel (0.7 ml $H_2O$, 3.0 ml 30% acrylamide mix) with a gradient mixer (Merck #Z340391). The rest of the gel components are the same like in Table 2.

**Table 2. Composition of SDS gel**

| | separating gel | | | | stacking gel | |
|---|---|---|---|---|---|---|
| | 6 % | | 8 % | | 4 % | |
| | 1x [5 ml] | 2x [10 ml] | 1x [5 ml] | 2x [10 ml] | 1x [5 ml] | 2x [10 ml] |
| H2O [ml] | 2.7 | 5.3 | 2.3 | 4.6 | 0.68 | 1.4 |
| 30 % acrylamide mix [ml] | 1.0 | 2.0 | 1.3 | 2.7 | 0.17 | 0.33 |
| 1.5 M Tris pH 8.8 [ml] | 1.3 | 2.5 | 1.3 | 2.5 | 0.13 | 0.25 |
| 10 % SDS [µl] | 50 | 100 | 50 | 100 | 10 | 20 |
| 10 % APS [µl] | 50 | 100 | 50 | 100 | 10 | 20 |
| TEMED [µl] | 4 | 8 | 3 | 6 | 1 | 2 |

After the gel is completely polymerized, the com was removed and the electrophoresis chamber was filled with 1 x running buffer (250 mM Tris, 192 mM glycine, 10% SDS for 10 x stock solution), including the sample slots. Subsequently, the gel was loaded with samples (including protein marker) and run with 100 V for 2 h until proteins are well separated.

At the end of the run, the cover glasses containing the SDS gel were slowly removed from the apparatus and temporarily laid into a bath of ice cold 1 x transfer buffer (250 mM Tris, 192 mM glycine for 10 x stock solution). The gel was carefully transferred onto a nitrocellulose paper and assembled with Whatman™ gel blotting paper (Sigma-Aldrich # WHA10547922) in a “blotting sandwich” (Fig. 5). In order to avoid faulty protein transfer through enclosed air bubbles, a falcon tube was carefully rolled over the assembled blotting sandwich. The gel cassette was put into the blotting tank and filled up with fresh transfer buffer. The protein transfer was run at 4°C under constant stirring with 350 mA.

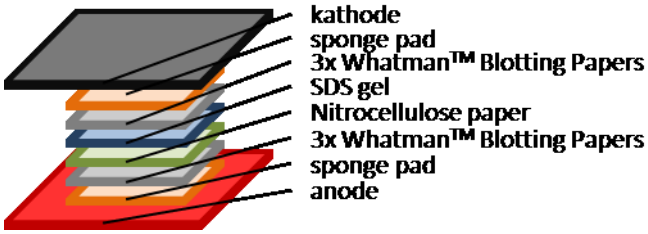


**Fig. 5.** Western Blot „blotting sandwich“

After the run, the nitrocellulose paper, together with the gel, was carefully removed from the blotting sandwich and overlaying paper was cut off with a scalpel. The bands of the marker were marked with a pen. Then, the blot was washed one time for 10 min with PBS + Tween 20 (0.1 % Tween 20 in 1x PBS) on a platform rotator. Afterwards, the blot was blocked with either 10 ml of 5 % milk (for antibody α20 and α74) or 5 % BSA (for antibody G10, Abcam, #ab78540) in PBS + Tween 20 for 1h at RT on the platform rotator. Subsequently, the first antibody was added to the blocking solution and incubated at 4°C overnight at the platform rotator.

The next day, the blocking solution was discarded (or can be stored at 4°C for an additional use) and washed three times with PBS + Tween 20. Each washing step was carried out at RT for 10 min and on the platform rotator. After the last washing step, 10 ml of PBS + Tween 20 together with a secondary HRP conjugated antibody (1:20,000) was added to the blot and incubated for 1 h at RT and the platform rotator. The blot was washed three times with PBS + Tween 20 afterwards.

The washed membrane was treated with SuperSignal™ West Pico PLUS Chemiluminescent Substrate kit (Thermo Fisher Scientific, # 34577). Therefore, a working solution was prepared by mixing equal parts of both solutions together and pipetted on the membrane (approximately 1 ml). The blot was incubated in the working solution at RT for at least on minute. Excess amounts of reagent were removed and the blot was placed on a clear plastic sheet on both sides. The blots were exposed to CL-XPosure™ Film 13 x 18 cm (Thermo Fisher Scientific, # 34090) in the darkroom.

## 2.12. Production of concentrated reelin and mock conditioned medium

HEK293 cells were seeded on 20 cm dishes with DMEM + 10 % FCS + 0.2 mg/ml G418 until 80 % confluence at 37°C and 5 % $CO_2$. For concentrated reelin conditioned medium

(cRCM), HEK293 cells were transfected with reelin plasmid. Otherwise, for mock conditioned medium (cMCM), wildtype HEK293 cells were used. 48 h before reelin collection, the medium was exchanged with Gibco™ OPTI-MEM™ (Thermo Fisher # 51985026) without FCS. Afterwards, the medium of reelin producing HEK cells was sterile filtrated, pipetted into Quick-seal™ tubes (Beckman Coulter # 342414 and # 342699) until completely full and ultra-centrifuged at 40000 x g overnight at 4°C. The next day the supernatant was carefully drained. The protein pellet was carefully collected with a syringe (with a dull needle) and stored in a microtube at -20°C (Fig. 6). [Brandes, et al; 2001]

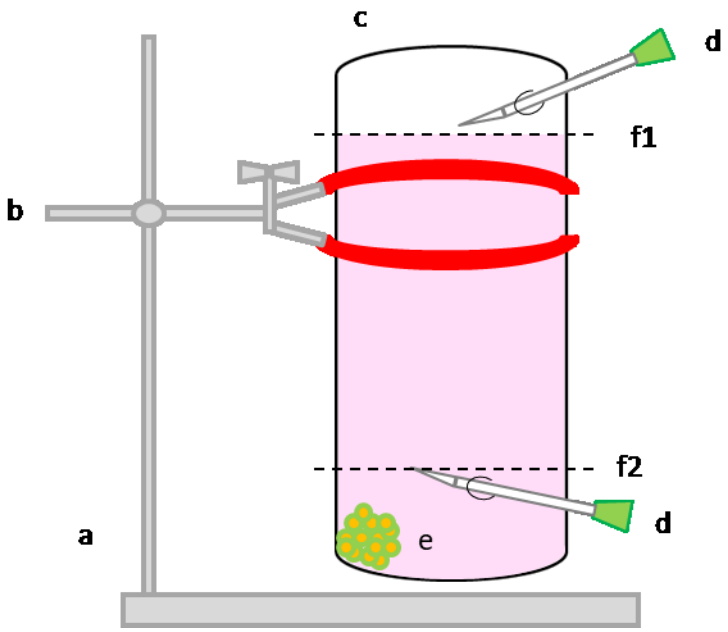


**Fig. 6**. Production of reelin. After centrifugation, the Quick-seal™ tube was punctured with a syringe needle above the level of the medium and above the protein pellet .After the medium drained completely (f2), the pellet was absorbed with another dull needle attached to a syringe. a: laboratory stand, b: tripod clam, c: Quick-seal™ tube, d: syringe needle, e: protein aggregate, f: level of medium (f1: start, f2: end).

## 2.13. PCR

Total RNA extracts were reverse transcribed via the Thermo Scientific DyNAmo cDNA Synthesis Kit (Thermo Scientific, #F-470L). Therefore, 2 µl [≈1 µg] of RNA template were added to a mixture of 10 µl of RT buffer (2x), 1 µl of random hexamer primer set (300 ng/µl) and 2 µl of M-MuLV RNase $H^+$ reverse transcriptase and filled up to a total volume of 20 µl with nuclease free $H_2O$. Primer extension was run at 25°C for 10 min followed by cDNA synthesis at 37°C for 30 min and a reaction termination step at 85°C for 5 min.

Two regions of reelin were amplified by PCR using four different primers RELN1#62 (5´-CAG TTG TGT GAA CAA GGA GC-3´), RELN1#63 (5´-GAT GAT TGT GCT GAC ATT GG-3`), RELN2#64 (5´-GAA GTG TTT CTC AGC CAT CT-3´) and RELN2#65 (5´-AGA GTG TGG GTC AAG TAG CA-3´). Primers were designed using primerblast (NCBI) and purchased by Eurofins Scientific SE. PCR was performed with the Q5™ High-Fidelity DNA Polymerase kit (NEB #M049G). One PCR reaction with a total volume 25 µl contained 5 µl 5x Q5 Reaction Buffer, 0.5 µl dNTPs (10mM), 1.25 µl forward and reverse primer each (10 µM), 5 µl Q5 High GC Enhancer, 0.25 µl Q5 High-Fidelity DNA Polymerase and 2 µl (≈1 µg) of cDNA Template. Reelin PCR was run at 98°C for 30 seconds followed by 35 cycles of 98°C for 10 seconds, 62°C for 30 seconds, 72°C for 20 seconds and finally 72°C for 2 minutes. Negative controls were included in every run. Products of PCR were analyzed on an agarose gel 1% in 1 x TAE Buffer with 5 µl Midori green and run for an hour with 100 V.

## 2.14. Microscopy

ApoER2 or VLDLR transfected cells were grown on sterile glass cover slips (coated with 40 µg/ml poly-L-lysine in PBS and incubated 1 h at 37°C) in a 24 well plate and treated with 200 µl imaging medium (Thermo Fisher Scientific, #A14291DJ) at 37°C and 5 % $CO_2$ for 1 h. Afterwards, 25 µl cMCM or cRCM were added and again incubated for 10 min at 37°C and 5 % $CO_2$.

The following steps were carried out on ice. The medium was aspirated, the cells were washed three times with ice cold PBS and fixed with formaldehyde, just enough to cover the cells (≈200µl per well). After an incubation time of 15 min at RT and darkness, the formaldehyde was aspirated and cells were washed again three times with PBS. In order to make the cell walls permeable, a solution of PBS + Tween 20 0.5 % was added and incubated 15 min at RT. Cells were washed three times with PBS and blocked with 1 % BSA for 30 min at RT. Now the first antibody was added (G10 1:1,000) and incubated at 4°C overnight on the platform rotator.

The next day, cells were washed three times with ice cold PBS. Then, a fluorescent secondary antibody (DyLight™ 633 goat anti mouse, 1:400, Thermo Fisher Scientific, #35512) was added and incubated 1 h at RT and darkness. Subsequently, the cells were washed with ice cold PBS again.

In the next step, the cells were treated with DAPI (5 µg/ml, Thermo Fisher Scientific, #D1306) and incubated for 5 min at RT and darkness. Again, the cells were washed three times with ice cold PBS. To achieve quenching of autofluorescence, cells were incubated with Glycin (100 mM) for 15 min at RT and darkness. The cover slips with the cells were mounted on microscope slide with either ibidi Mounting Medium (ibidi, #50001) or VECTASHIELD Antifade Mounting Medium (Vectorlabs, #H-1000) and fixed with a little nail polish. It was allowed to dry overnight at RT and then stored at 4°C.

Confocal laser microscopy was done with the LSM 700 from Zeiss and analyzed with ImageJ.

# 3 Results

## 3.1. ApoER2 detection in vivo reveals possible candidate for precursor.

First, the expression of ApoER2 pattern was examined by WB in whole tissue extracts an in cells transfected with plasmids coding for different variants of the receptor. Two different cell lines were transfected with full length ApoER2 and the brain of a 17 day old rat embryo was lysed. Afterwards, expression of ApoER2 was evaluated with two different antibodies. Both antibodies highlighted 3 distinguishable bands of ApoER2 in the rat brain extract with the relative molecular weight of 130 kDa, 115 kDa and 100 kDa (Fig. 7 A). In contrast, the cell lines expressed only 2 variants of the receptor migrating with relative molecular weights of 130 kDa and 115 kDa (Fig. 7 B). Usually, precursor proteins are not yet modified by post-translational modifications which occur on their way through the Golgi apparatus. This includes protein glycosylation and structural changes. Therefore, you would not expect precursor proteins to appear on the cell surface.

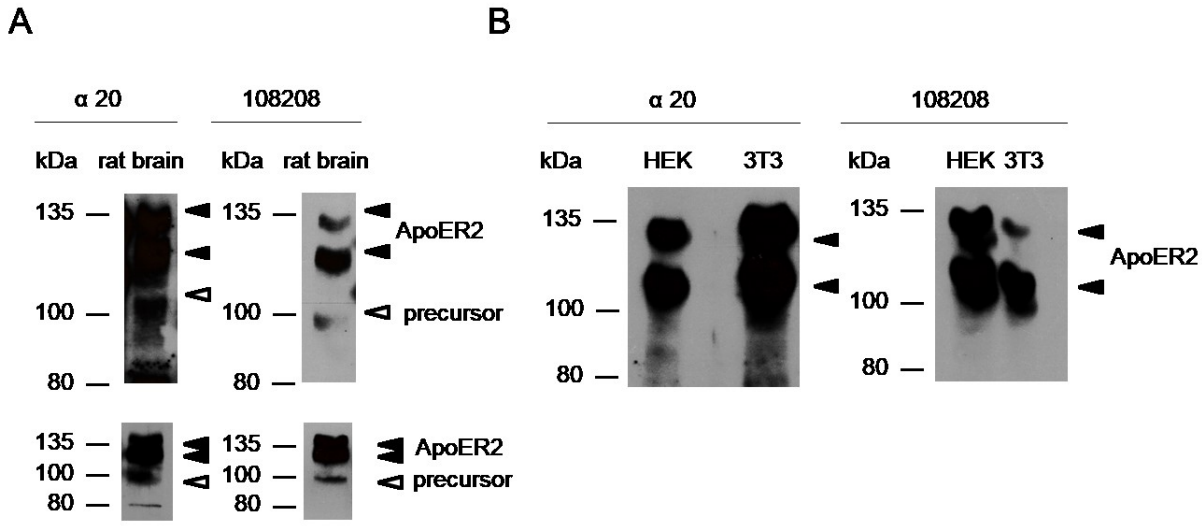


**Fig. 7.** Western Blots of ApoER2 HEK 292 and rat brain lysates. A: ApoER2 was extracted from embryonic rat brain tissue with 1-2 ml NP-40 lysis buffer. Proteins were separated in a 4.5% SDS separating gel (top) and a 4.5 % to 18 % gradient gel (bottom) and analysed by Western blotting with indicated antibodies (see methods). Closed arrows correspond to mature ApoER2 and open arrows correspond to hypothetical precursor of ApoER2. B: ApoER2 expressed in HEK and NIH3T3 cells transfected with pClneo_ApoER2 by incubating them with PEI (1µg/µl) in DMEM w/o FCS. After an incubation time of 24 h they were lysed with NP-40

lysis buffer. Proteins were separated in 4.5 % SDS separating gel. They were analysed by Western blotting with the indicated antibodies (see methods). Closed arrows correspond to mature ApoER2. Working concentration for α20 was 1:8,000 and for 108208 was 1:1,000.

## 3.2. Glycosylation does not influence receptor stability on the cell surface

In 2014, a Group of the Georgetown University Medical Center discovered that two variants of ApoER2 become labelled by a surface biotinylation. They hypothesized that the second band is the precursor of ApoER2 and was able to migrate to the cell surface due to protein overexpression. They supported their claim by the observation that the lower band (the putative precursor) was labelled to a significant lesser extent than the mature protein. The amount of both variants estimated by WB of whole cell extracts, however, showed similar amounts of both variants present [Burrell, et al; 2014]. Since the structure of ApoER2 is known (Fig. 8 D) [Kim, et al; 1997] it can be easily determined whether the second band is a glycosylated isoform or the non-glycosylated precursor by deleting the O-link sugar domain containing exon 16. Therefore, HEK 293 cells and CHO cells were transfected with plasmids coding for full length ApoER2 and for a variant lacking exon 16 coding for the O-linked sugar domain. Subsequently, a biotinylation experiment was carried out. Negative controls (unspecific beads, no biotin solution) were done for each experiment (Fig. 8 A&B lane 1&2 and lane 5&6). When the full length version of the receptor was expressed in HEK and CHO cells again two bands were labelled with apparent relative molecular masses of 130 and 115 kDa, respectively, in the lysate and after biotin labelling of cell surface proteins. Therefore, both variants of the ApoER2 (130 kDa and 115 kDa) are implemented in the cell membrane (Fig. 8 A&B Lane 4&8). Interestingly, the same is true for the truncated ApoER2Δ16 missing the O-linked sugar domain (Fig. 8 A&B Lane 3&7). Nevertheless, the truncated version migrates with an apparent relative molecular weight below 100 kDa which is lower than the lower band produced by full length ApoER2. The calculated weight of ApoER2 (sequence only) is 105.65 kDa and the calculated weight ApoER2Δ16 is 99.1 kDa resulting in a difference of 7.7 kDa. Taken together, its relative molecular mass and the observation that the receptor is located at the cell membrane suggest that the variant which lacks the O-linked sugar domain and thus is not glycosylated is still transported t and integrated into the cell membrane and that glycosylation is not necessary for membrane integration. This allows the conclusion that the 115 kDa ApoER2 may be a hypoglycosylated isoform. Additionally,

the truncated ApoER2 expressed in HEK293 cells has the same relative molecular mass as the variant seen as fastest migrating band in extracts derived from whole brain extracts.

Furthermore, another band appeared below 75 kDa. This band, however, could be only observed in lysates of HEK293 cells. It can be considered to represent either an unidentified protein cross reacting with the used antibody or a proteolytic fragment of the receptor.

Another interesting observation was that the bands with the lower protein weight (possible less glycosylation) in the Western Blots of the surface biotinylation experiments are less stable than the hyperglycosylated form of the receptor. This was also observed in a previous study, where it was postulated that the glycosylation protects the receptor from proteolytic cleavage [Wasser, et al; 2014]. Therefore, the loss of the Exon 16 or an altered glycosylation of the receptor could make the protein sensitive against proteases. In order to proof this, the biotinylation experiment was repeated with the full length receptor and with two different lysis buffers. One was containing freshly prepared protease inhibitors, whereas another one contained no protease inhibitor at all. The Western Blot revealed that the presence of protease inhibitor during cell lysis has a direct influence on the signal strength of the faster migrating band (Fig. 8 C). This allows three possible explanations. First, if both forms become degraded by the protease with the same efficiency. The cells have to produce more of the fully glycosylated receptor than the hypoglycosylated form. Second, the lower glycosylation level reduces the integration into the cell membrane. This can be ruled out as the truncated ApoER2Δ16 was also found on the cell surface. Therefore, glycosylation did not have an influence on integration into cell membrane. Third, the glycosylation does indeed hide a glycosylation side, making the less glycosylated receptor more vulnerable to proteolytic cleavage.

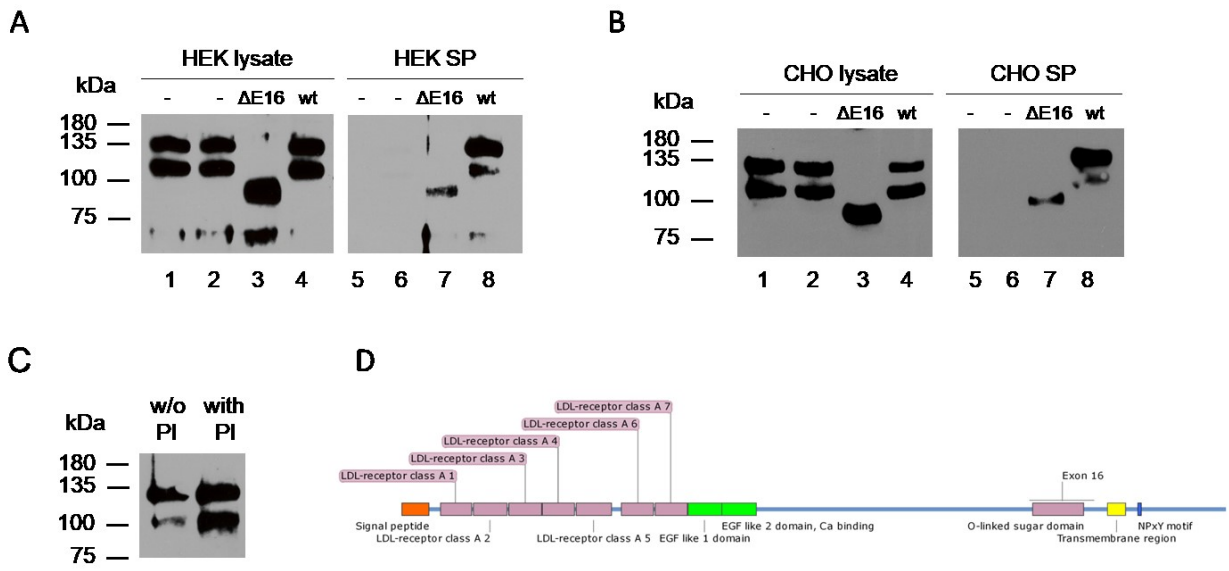


**Fig. 8.** Surface biotinylation of ApoER2. CHO and HEK 293 cells were transfected with plasmids coding for full length ApoER2 and a variant lacking exon 16. Biotinylation of surface proteins was performed as described in Materials and Methods. Cell extracts were prepared and proteins were separated by SDS-PAGE in 6% gels. WB was performed using the α20 antibody and the corresponding secondary antibody. A: Biotinylation HEK cells. B: Biotinylation CHO cells. C: Surface biotinylation of HEK cells with and without protease inhibitor. HEK cells were lysed with freshly prepared NP-40 lysis buffer. D: Schematic structure of ApoER2 (drawn with SnapGene, Sequence taken from NCBI #BAA21824).

## 3.3. Endogenous expression of reelin in HEK 293 cells

In the course of the study, reelin was produced as recombinant protein for microscopy experiment to locate reelin-receptor binding on the cell surface. Therefore HEK293 cells were transfected with a reelin encoding plasmid and cultured for 24 hours. Afterwards, the medium was exchanged with DMEM and the secreted reelin was concentrated (see methods) to obtain concentrated reelin conditioned medium. The same was done with non-transfected cells (concentrated mock conditioned medium) for control experiments. Interestingly, it was observed that both, cells which were treated with medium containing reelin and cells which were treated with mock medium showed reelin binding (Fig. 9 A&B).

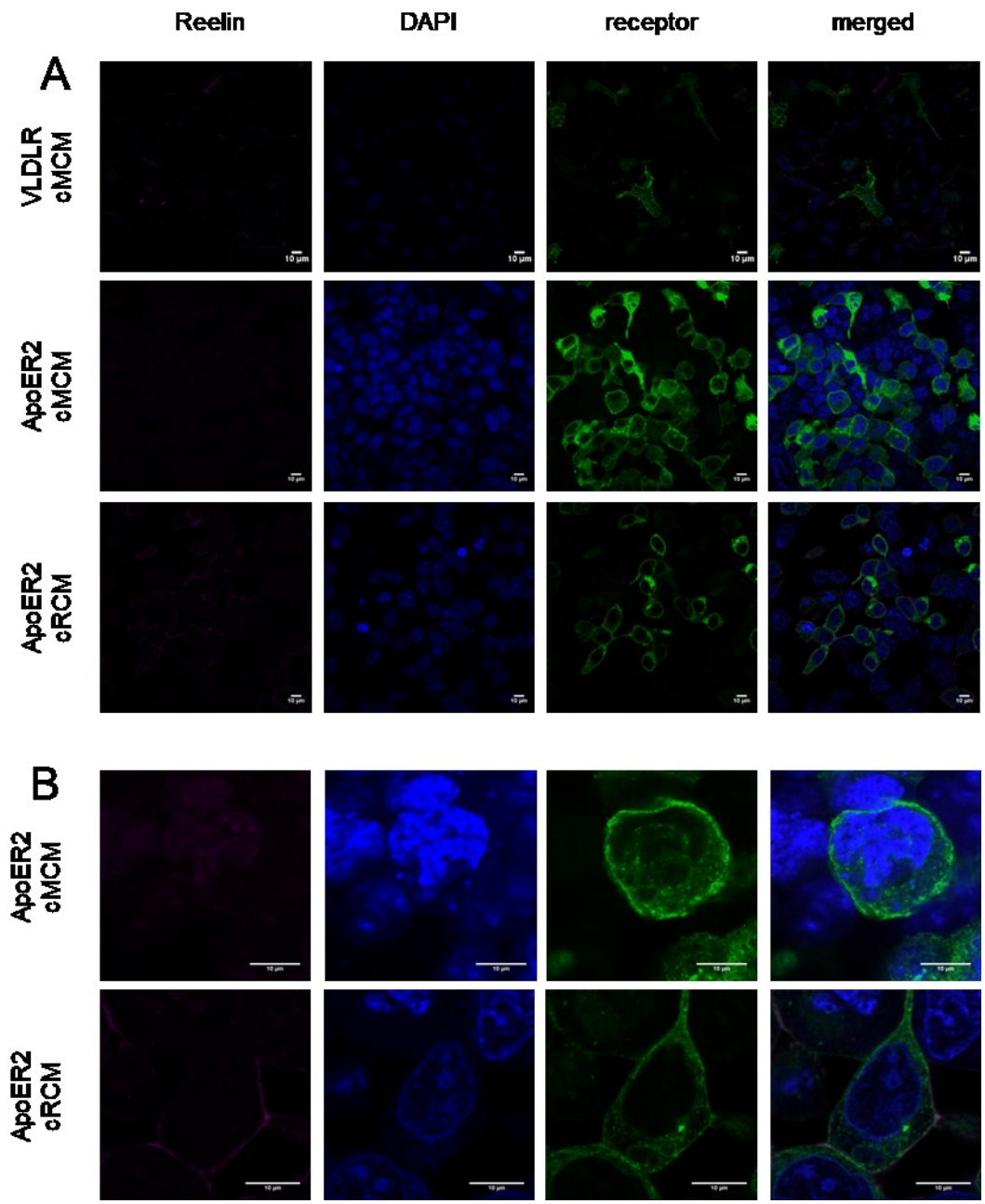


**Fig. 9.** Confocal Microscopy of HEK293 cells expressing an mGFP_ApoER2 or mGFP_VLDLR hybrid protein which were incubated with cRCM or cMCM for 24 h. Cells were fixed, permeabilized, and stained using G10 (1:1,000) for reelin detection. A: Overview of HEK 293 cells expressing ApoER2 or VLDLR treated with cRCM or cMCM. B: Single cell view of ApoER2 or VLDLR expressing cell treated with cRCM or cMCM. Bar size 10µm.

Western blotting of concentrated mock condition medium showed that it contained a truncated version of reelin termed N-R6 and N-R2 (Fig 9 A) [Yossin, et al; 2004]. This may indicate an intrinsic expression of reelin in HEK 293 cells. To test this assumption, HEK293

cells were seeded on 20 cm dishes and harvested after 24h and 96h. Afterwards, expression of reelin mRNA was verified via an RT- PCR experiment (Fig. 10 B).

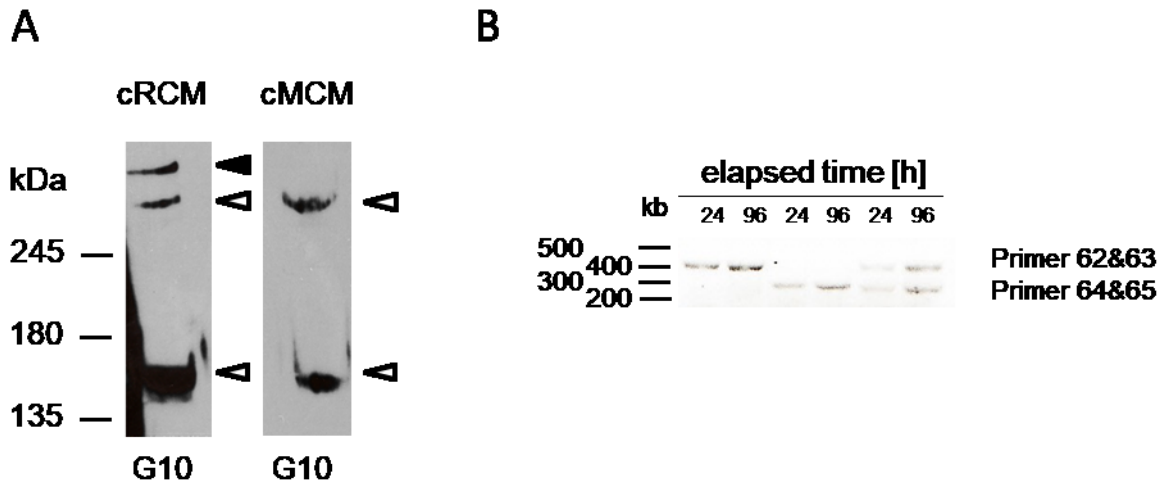


**Fig. 10.** Detection of reelin with Western Blotting and PCR. A: HEK293 cells with and without reelin plasmid were incubated with OPTI-MEM$^{TM}$ medium w/o FCS. Afterwards, secreted proteins were concentrated and extracted. Content of the medium were separated by 4.5% SDS gels and analysed by Western blotting using the indicated antibody (G10 1:10,000) and the corresponding goat anti-mouse secondary antibody. Closed arrows correspond to full length reelin and open arrows correspond to truncated reelin N-R6 and N-R2. B: In order to detect reelin in wildtype HEK cells mRNA was extracted at different time points (24 and 96 h) and reverse transcribed. Afterwards, reelin mRNA was amplified with two different sets of primer pairs (see methods). Expected product size was 405 and 259 kb.

In order to exclude the possibility of genomic contamination in the PCR reaction, the primer pairs were chosen in a way that they are located in exons with at least one intron in between. Using cDNA originated from mRNA as template, primers # 62 and # 63 amplified a 405 bp long product, whereas #64 and #65 give a product with a length of 259 bp (Fig. 11 B) (NCBI RefSeq. reelin mRNA NM_005045.3). In contrast, using genomic DNA as template primer #62 and #63 would form a 78,510 bp large piece of DNA (NCBI RefSeq reelin NG_011877.1) and primer #64 and #65 would produce a piece of DNA with a length of 2352 bp (Fig. 11 A). In summary, it can be assumed that HEK293 cells contain small amounts of reelin mRNA. Even if the presence of the full length protein could not be verified with WB,

PCR experiments showed that mRNA is present. The mRNA of the alternative spliced reelin variants N-R6 and N-R2 would not give a PCR signal with the second primer pair.

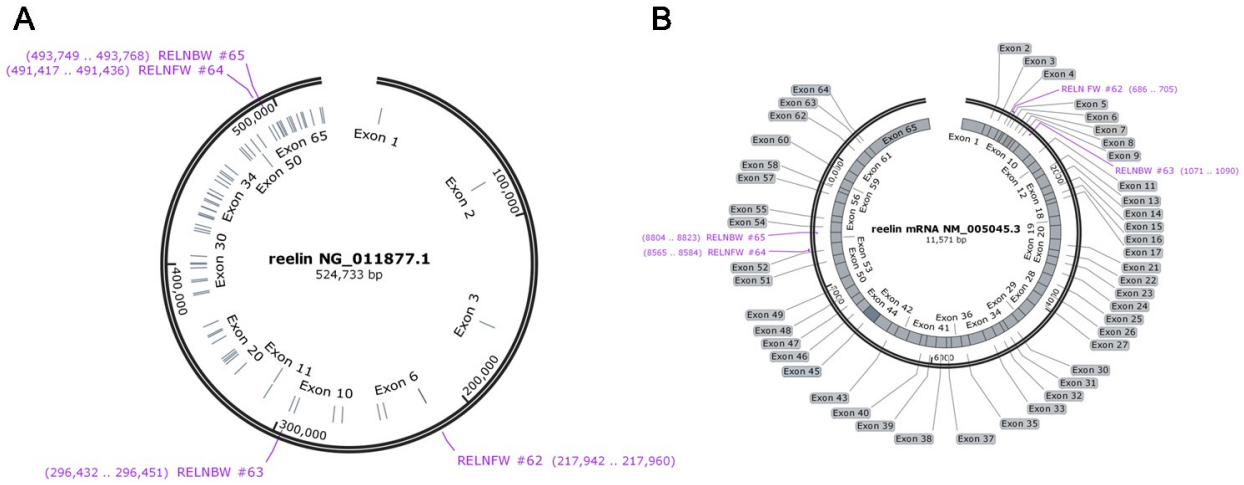


**Fig. 11.** Organization of the reelin gene. A: reelin gene genomic DNA NCBI Accession Number NG_011877.1 containing a total of 524,733 bp with 65 Exons. Primer #62 extends from bp 217,942 to 217,960 and primer #63 extends from bp 296,432 to 296,451 resulting in a hypothetical 78,510 bp product. Primer #64 extends from bp 491,417 to 491,436 and primer #65 extends from bp 493,749 to 493,768 resulting in a hypothetical 2,352 bp product. B: reelin mRNA NCBI Accession Number NM_005045.3 containing a total of 11,571 bp. Primer #62 extends from bp 686 to 705 and primer #63 extends from bp 1,071 to 1,090 resulting in a 405 bp PCR product. Primer #64 extends from bp 8565 to 8584 and primer #65 extends from bp 8804 to 8823 resulting in a 2,352 bp PCR product. Figure was created with SnapGene.

.

# 4 Discussion

Summarizing the results, it can be confirmed that two different types of ApoER2 exist and are localized in the cell membrane. In order to confirm or disprove the 115 kDa ApoER as the precursor, pulse chase experiments with radioactively labeled $^{35}$S methionine and $^{35}$S cysteine were carried out in our laboratory by Paula Dlugosz. Therefore, ApoER2 transfected HEK 293 cells were treated with the radioactive amino acids in order to label the newly synthesized proteins. Afterwards, the radioactive solution was replaced with complete media. Thereby, newly synthesized proteins have no radioactive label. In such an experiment, the radioactive label of the precursor would vanish over time. However, the results showed that the signal of the 115 kDa band remained over time. Consequently, the second band cannot be the ApoER2 precursor.

Experiments analyzing ApoER2 variants in rat brain tissue showed an additional band that cannot be detected in vitro under the same conditions. HEK293, NIH3T3 and CHO cells show no third band in a Western Blot in vitro. Since the receptor of in vitro studies is expressed from a plasmid and thus is not affected by alternative splicing, it cannot be said with certainty if the 100 kDa in vivo band is the ApoER2 precursor or a tissue/development specific isoform that is expressed during early brain development only.

Previous studies carried out to locate the ApoER2 in the cell membrane by density centrifugation showed that that the upper band, at approximately 130 kDa, is located in lipid rafts, whereas the lower one at approximately 115 kDa is not. It was hypothesized that the lower one is the precursor and therefore not on the cell surface, but still in the Golgi apparatus [Duit, et al; 2010]. In contrast, biotinylation experiments done during this thesis revealed that the 115 kDa receptor is embedded in the cell membrane. This would lead to the conclusion, that the lower band at 115 kDa is not the precursor (see above, pulse chase experiments) but a mature variant which is exclusively located in the non-lipid raft fraction of the cell membrane. This could be proven by an additional density centrifugation experiment. Furthermore, since the VLDLR is also not located in the lipid rafts [Duit, et al; 2010] but is known to form clusters with ApoER2 when reelin is bound [Strasser, et al; 2004] it could mean that the second band is a new isoform of ApoER2 exclusively forming heterodimers with VLDR, whereas the 130 kDa receptor is only able to form homodimers. This would also indicate that different functions of the variants are conceivable.

The observation that the 115 kDa band is less abundant on the cell surface could not be observed. [Wasser, et al; 2014] In contrary, under protease inhibiting conditions, the quantity of both receptor variants seemed to be the same. Without protease inhibitors the lower band is diminished most likely due to proteolytic degradation. This could indicate, that it is more accessible to proteases due to the lack of glycosylation as mentioned by Wasser et al (Wasser, et al; 2014) or the cell produces more of the 130 kDa receptor. This could be confirmed by repeating the experiment with a glycosylation deficient cell line.

Furthermore, expression of a receptor variant lacking exon 16 which is coding for the O-linked sugar domain in combination with biotinylation experiments revealed that no glycosylation of the receptor is needed to be transported and integrated in the cell membrane.

Since a lot of experiments regarding the reelin signaling pathway are done with HEK 293 cells, it is important that their proteome is well known. It could be shown that wildtype HEK293 cells contain copies of reelin mRNA. Since the results from microscopy experiments are not significant enough, it cannot be said with certainty whether this mRNA is transcribed into functional protein. Even if reelin could be detected with WB in HEK wildtype, no full length reelin could be observed. However, this could be due to small proteins amounts. Therefore, wild type HEK cells should be analyzed for reelin with protein mass spectroscopy.

# 5 References


1. **Ballard C, Gauthier S, Corbett A, Brayne C, Aarsland D, Jones E**. Alzheimer's disease. Lancet. 2011 Mar 19;377(9770):1019-31. doi: 10.1016/S0140-6736(10)61349-9. Epub 2011 Mar 1.

2. **Biggerstaff KD, Wooten JS**. Understanding lipoproteins as transporters of cholesterol and other lipids. Adv Physiol Educ. 2004 Dec;28(1-4):105-6.

3. **Brandes C, Kahr L, Stockinger W, Hiesberger T, Schneider WJ & Nimpf J**. Alternative splicing in the ligand binding domain of mouse ApoE receptor-2 produces receptor variants binding reelin but not alpha 2-macroglobulin. J Biol Chem. 2001 Jun 22;276(25):22160-9. Epub 2001 Apr 6.

4. **Botella-López A, Burgaya F, Gavín R, García-Ayllón MS, Gómez-Tortosa E, Peña-Casanova J, Ureña JM, Del Río JA, Blesa R, Soriano E, Sáez-Valero J**. Reelin expression and glycosylation patterns are altered in Alzheimer's disease. Proc Natl Acad Sci U S A. 2006 Apr 4;103(14):5573-8. Epub 2006 Mar 27.

5. **Burrell TC, Divekar SD, Weeber EJ, Rebeck GW.** Fyn tyrosine kinase increases Apolipoprotein E Receptor 2 levels and phosphorylation. PLoS One. 2014 Oct 23;9(10):e110845. doi: 10.1371/journal.pone.0110845. eCollection 2014.

6. **Duit S, Mayer H, Blake SM, Schneider WJ, Nimpf J.** Differential functions of ApoER2 and very low density lipoprotein receptor in Reelin signaling depend on differential sorting of the receptors. J Biol Chem. 2010 Feb 12;285(7):4896-908. doi: 10.1074/jbc.M109.025973. Epub 2009 Nov 30.

7. **Durrington, P**. Dyslipidaemia. Lancet. 2003 Aug 30;362(9385):717-31. doi: 10.1016/S0140-6736(03)14234-1

8. **Frotscher M**. Cajal-Retzius cells, Reelin, and the formation of layers. Curr Opin Neurobiol. 1998 Oct;8(5):570-5.

9. **Go GW, Mani A**. Low-density lipoprotein receptor (LDLR) family orchestrates cholesterol homeostasis. Yale J Biol Med. 2012 Mar;85(1):19-28. Epub 2012 Mar 29.

10. **Hayashi K, Nimpf J, Schneider WJ.** Chicken oocytes and fibroblasts express different apolipoproteins-B-specific receptors. J Biol Chem. 1989 Feb 25;264(6):3131-9.

11. **Haydar TF, Blue ME, Molliver ME, Krueger BK, Yarowsky PJ**. Consequences of trisomy 16 for mouse brain development: corticogenesis in a model of Down syndrome. J Neurosci. 1996 Oct 1;16(19):6175-82.

12. **Honda T, Kobayashi K, Mikoshiba K, Nakajima K**. Regulation of cortical neuron migration by the reelin signaling pathway. Neurochem Res. 2011 Jul;36(7):1270-9. doi: 10.1007/s11064-011-0407-4. Epub 2011 Jan 21.

13. **Huang GN**. Biotinylation of Cell Surface Proteins. Bio-protocol 2(9): e170. DOI: 10.21769/BioProtoc.170.

14. **Ishii K, Kubo KI, Nakajima K.** Reelin and Neuropsychiatric Disorders. Frontiers in cellular neuroscience. Front Cell Neurosci. 2016 Oct 18;10:229. eCollection 2016.

15. **Jossin Y, Ignatova N, Hiesberger T, Herz J, Lambert de Rouvroit C, Goffinet AM.** The central fragment of Reelin, generated by proteolytic processing in vivo, is critical to its function during cortical plate development. J Neurosci. 2004 Jan 14;24(2):514-21.

16. **Kim DH, Magoori K, Inoue TR, Mao CC, Kim HJ, Suzuki H, Fujita T, Endo Y, Saeki S, Yamamoto TT.** Exon/intron organization, chromosome localization, alternative splicing, and transcription units of the human apolipoprotein E receptor 2 gene. J Biol Chem. 1997 Mar 28;272(13):8498-504.

17. **Lane-Donovan C, Herz J**. The ApoE receptors Vldlr and ApoEr2 in central nervous system function and disease. J Lipid Res. 2017 Jun;58(6):1036-1043. doi: 10.1194/jlr.R075507. Epub 2017 Mar 14.

18. **Lane-Donovan C, Herz J**. ApoE, ApoE Receptors, and the Synapse in Alzheimer's Disease. Trends Endocrinol Metab. 2017 Apr;28(4):273-284. doi: 10.1016/j.tem.2016.12.001. Epub 2017 Jan 2.

19. **Li Y, Lu W, Marzolo MP, Bu G**. Differential functions of members of the low density lipoprotein receptor family suggested by their distinct endocytosis rates. J Biol Chem. 2001 May 25;276(21):18000-6. Epub 2001 Feb 21.

20. **Marais AD**. Familial Hypercholesterolaemia. In: Clin Biochem Rev. 25(1), S. 49–86.

21. **Nes DW**. Biosynthesis of cholesterol and other sterols. Chem Rev. 2011 Oct 12;111(10):6423-51. doi: 10.1021/cr200021m. Epub 2011 Sep 8.

22. **Nykjaer A, Willnow TE**. The low-density lipoprotein receptor gene family: a cellular Swiss army knife? Trends Cell Biol. 2002 Jun;12(6):273-80.

23. **Parthasarathy S, Raghavamenon A, Garelnabi MO, Santanam N**. Oxidized low-density lipoprotein. Methods Mol Biol. 2010;610:403-17. doi: 10.1007/978-1-60327-029-8_24.

24. **Peng J, Luo F, Ruan G, Peng R, Li X.** Hypertriglyceridemia and atherosclerosis. Lipids Health Dis. 2017 Dec 6;16(1):233. doi: 10.1186/s12944-017-0625-0.

25. **Quattrocchi CC, Wannenes F, Persico AM, Ciafré SA, D'Arcangelo G, Farace MG, Keller F**. Reelin is a serine protease of the extracellular matrix. J Biol Chem. 2002 Jan 4;277(1):303-9. Epub 2001 Oct 31.

26. **Raal FJ, Santos RD.** Homozygous familial hypercholesterolemia: current perspectives on diagnosis and treatment. Atherosclerosis. 2012 Aug;223(2):262-8. doi: 10.1016/j.atherosclerosis.2012.02.019. Epub 2012 Feb 16.

27. **Reddy SS, Connor TE, Weeber EJ, Rebeck W**. Similarities and differences in structure, expression, and functions of VLDLR and ApoER2. Mol Neurodegener. 2011 May 9;6:30. doi: 10.1186/1750-1326-6-30.

28. **Rohani N, LCanty L, Luu O, Fagotto F, Winklbauer R.** EphrinB/EphB signaling controls embryonic germ layer separation by contact-induced cell detachment. PLoS Biol. 2011 Mar;9(3):e1000597. doi: 10.1371/journal.pbio.1000597. Epub 2011 Mar 1.

29. **Schneider WJ, Nimpf J**. LDL receptor relatives at the crossroad of endocytosis and signalling. Cell Mol Life Sci. 2003 May; 60(5):892-903.

30. **Stifani S, Barber DL, Aebersold R, Steyrer E, Shen X, Nimpf J, Schneider WJ.** The laying hen expresses two different low density lipoprotein receptor-related proteins. J Biol Chem. 1991 Oct 5;266(28):19079-87.

31. **Stockinger W, Brandes C, Fasching D, Hermann M, Gotthardt M, Herz J, Schneider WJ, Nimpf J.** The reelin receptor ApoER2 recruits JNK-interacting proteins-1 and -2. J Biol Chem. 2000 Aug 18;275(33):25625-32.

32. **Strasser V, Fasching D, Hauser C, Mayer H, Bock HH, Hiesberger T, Herz J, Weeber EJ, Sweatt JD, Pramatarova A, Howell B, Schneider WJ, Nimpf J.** Receptor Clustering Is Involved in Reelin Signaling. Mol Cell Biol. 2004 Feb;24(3):1378-86.

33. **Tissir F, Goffinet AM**. Reelin and brain development. Nat Rev Neurosci. 2003 Jun;4(6):496-505. doi: 10.1038/nrn1113

34. **Trommsdorff M, Gotthardt M, Hiesberger T, Shelton J, Stockinger W, Nimpf J, Hammer RE, Richardson JA, Herz J**. Reeler/Disabled-like disruption of neuronal

migration in knockout mice lacking the VLDL receptor and ApoE receptor 2. Cell. 1999 Jun 11;97(6):689-701.

35. **Wasser CR, Masiulis I, Durakoglugil MS, Lane-Donovan C, Xian X, Beffert U, Agarwala A, Hammer RE, Herz J.** Differential splicing and glycosylation of Apoer2 alters synaptic plasticity and fear learning. Sci Signal. 2014 Nov 25;7(353):ra113. doi: 10.1126/scisignal.2005438.

36. **Weeber EJ, Beffert U, Jones C, Christian JM, Forster E, Sweatt JD, Herz J**. Reelin and ApoE receptors cooperate to enhance hippocampal synaptic plasticity and learning. J Biol Chem. 2002 Oct 18;277(42):39944-52. Epub 2002 Aug 7. doi:10.1074/jbc.M205147200

37. **Yu NN, Tan MS, Yu JT, Xie AM, Tan L**. The Role of Reelin Signaling in Alzheimer's Disease. Mol Neurobiol. 2016 Oct;53(8):5692-700. doi: 10.1007/s12035-015-9459-9. Epub 2015 Oct 21.
38. **Zhao S, Frotscher M**. Go or stop? Divergent roles of Reelin in radial neuronal migration. Neuroscientist. 2010 Aug;16(4):421-34. doi: 10.1177/1073858410367521.

39. **Zmysłowski A, Szterk A.** Current knowledge on the mechanism of atherosclerosis and pro-atherosclerotic properties of oxysterols. Lipids Health Dis. 2017 Oct 2;16(1):188. doi: 10.1186/s12944-017-0579-2.